

Photon Bubble Turbulence in Cold Atomic Gases

João D. Rodrigues,^{1,*} José A. Rodrigues,^{2,1} António V. Ferreira,¹ Hugo Terças,³ Robin Kaiser,⁴ and José T. Mendonça¹

¹*Instituto de Plasmas e Fusão Nuclear, Instituto Superior Técnico, Universidade de Lisboa, 1049-001 Lisbon, Portugal*

²*Departamento de Física, Faculdade de Ciências e Tecnologia, Universidade do Algarve, 8005-139 Faro, Portugal*

³*Physics of Information and Quantum Technology Group, Instituto de Telecomunicações, Lisbon, Portugal*

⁴*Institut Non Linéaire de Nice, CNRS and Université Nice Sophia Antipolis, 1361 route des Lucioles, 06560 Valbonne, France*

Turbulent radiation flow is ubiquitous in many physical systems where light-matter interaction becomes relevant. Photon bubbling, in particular, has been identified as the main source of turbulent radiation transport in many astrophysical objects, such as stars and accretion disks. This mechanism takes place when radiation trapping in optically dense media becomes unstable, leading to the energy dissipation from the larger to the smaller bubbles. Here, we report on the observation of photon bubble turbulence in cold atomic gases in the presence of multiple scattering of light. The instability is theoretically explained by a fluid description for the atom density coupled to a diffusive transport equation for the photons, which is known to be accurate in the multiple scattering regime investigated here. We determine the power spectrum of the atom density fluctuations, which displays an unusual k^{-4} scaling, and entails a complex underlying turbulent dynamics resulting from the formation of dynamical bubble-like structures. We derive a power spectrum from the theoretical photon bubble model which, to a high level of accuracy, explains the observations. The experimental results reported here, along with the theoretical model we developed may shed light on the analogue photon bubble instabilities in astrophysical scenarios.

PACS numbers: 37.10.Vz, 52.35.Ra, 47.27.-i

Due to multiple scattering in dense astrophysical systems such as massive stars, light propagation is often diffusive instead of ballistic. In such optically thick media, photons exhibit high residence times and can therefore be trapped [1]. One interesting consequence of such diffusive behaviour is the so-called photon bubbling [2], an effect that is possible when the system dynamically responds to the propagation of light. Photon bubbling consists in the formation and growth of light bubbles that eventually leave the medium or decay into smaller bubbles. This decay is at the origin of a specific form of turbulence in optically thick media, the photon bubble turbulence (PBT). Interestingly, the PBT spectrum significantly differs from the usual Kolmogorov (or similar) decay cascades, which scale as $\sim k^{-5/3}$. Physically, the mechanism leading to turbulence is the saturation of the photon-bubbling instability, and the corresponding decay spectrum strongly depends on the optical properties of the media.

In this Letter, we reveal the experimental evidence of a photon bubble instability in an optically thick, cloud of cold atoms driven close to the atomic resonance, conditions under which diffusive photon transport takes place [3–5]. We determine the spectrum of the density fluctuations, which we compare with an extension of a previously developed model of photons bubbles. The obtained theoretical spectral dependence, which significantly differs from the Kolmogorov case, is shown to accurately

describe all the features of the observed turbulence spectrum. We start by briefly introducing a fluid model for the cold atoms in a laser trap, revealing the essential ingredients for the photon bubble instability. We describe the experimental set-up and the conditions under which such instability is observed. The turbulence spectrum is measured and compared to the theory developed here. A detailed analysis of the results is presented before stating some final conclusions.

For conditions of high optical densities and near resonant driving, the laser cooling beams are deflected by multiple scattering inside the medium, randomizing the photon propagation direction thus turning photon transport into an isotropic diffusive process described by [6, 7]

$$\frac{\partial}{\partial t} I - \nabla \cdot (D \nabla I) = -\gamma_a I, \quad (1)$$

where I is defined as the spectral energy density of the electromagnetic radiation field $W(\omega, \mathbf{k})$, integrated over all possible directions of propagation and $\gamma_a = D k_a^2$ with k_a the inverse of the energy absorption length. The photon mean free path $l = 1/n\sigma_L$, with n the atom density and σ_L the photon absorption cross-section, determines the light diffusion coefficient as $D = l^2/\tau$. The photon diffusion time, τ , is usually considered independent from the atom density [8], yielding a dependence of the form $D \propto n^{-2}$ while providing a strong coupling between the atom dynamics and photon transport. On the other side, the atom density n and the velocity field \mathbf{v} are determined by the usual continuity and Navier-Stokes

* Corresponding author: joaodmrodrigues@tecnico.ulisboa.pt

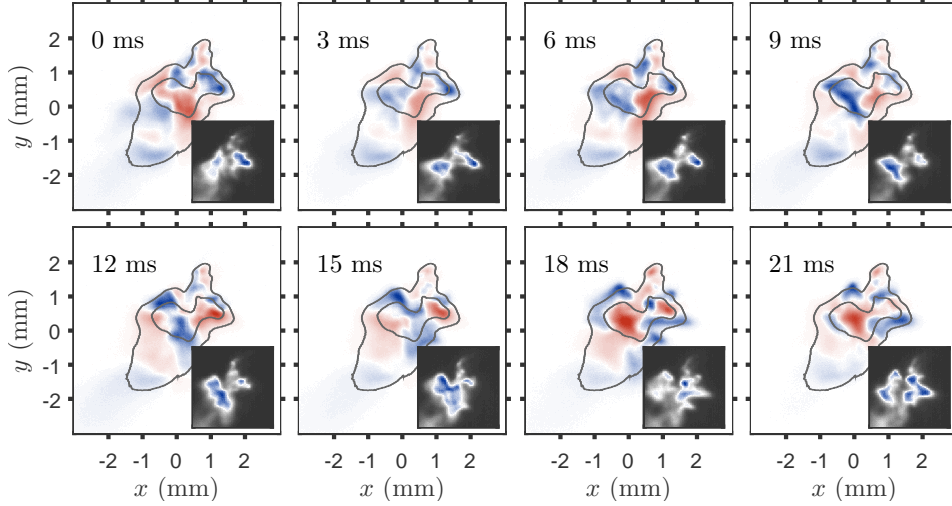


FIG. 1. (color online) Temporal evolution of the turbulent phase, after the photon bubble instability is fully developed. The plots corresponds to the fluorescence signal (proportional to the atom density, integrated along the line-of-sight) fluctuations - for each frame the average density profile, computed with as many as 500 frames, is subtracted. The blue and red colors then represent regions of higher and lower densities than the local average density, respectively. The grey counters corresponds to level lines of the average density, thus representing the shape of the average atom distribution. The inset plot depicts the real atom density distribution (integrated along the line-of-sight of the camera) without the subtracted averaged, in false color code (blue regions correspond to high atom densities).

equations

$$\frac{\partial n}{\partial t} + \nabla \cdot (n\mathbf{v}) = 0, \quad \text{and} \quad (2)$$

$$\frac{\partial \mathbf{v}}{\partial t} + (\mathbf{v} \cdot \nabla)\mathbf{v} = \frac{\mathbf{F}}{m} - \frac{\nabla P}{nm} - \nu\mathbf{v}, \quad (3)$$

respectively, where P is the thermodynamical pressure, ν the damping rate from optical molasses and m the atom mass. In the presence of multiple scattering of light a radiation pressure force scaling as $1/r^2$ appears due to exchange of photons between nearby atoms. This collective force \mathbf{F} is determined by a Poisson-like equation,

$$\nabla \cdot \mathbf{F} = Qn, \quad (4)$$

where $Q = (\sigma_R - \sigma_L)\sigma_L I/c$ is related to an effective electrical charge for the atoms and σ_L and σ_R are the atom-photon absorption and re-emission cross-sections, respectively [3, 9]. This suggests the introduction of an effective plasma frequency, $\omega_p = \sqrt{Qn_0/m}$ [4, 5], and allows for an analogy with an electrostatically self interacting one-component trapped plasma, which has been explored before in the context of exotic phenomena such as classical rotons [10] or instability of twisted excitations [11]. In typical experimental conditions [12, 13] the effective charge is of the order $q = \sqrt{\epsilon_0 Q} \sim 10^{-4}e$, with e the electron charge, and the atom densities $n_0 \sim 10^{10} \text{ cm}^{-3}$, resulting in plasma frequencies of the order $\omega_p \sim 100 - 200 \text{ Hz}$. Notice that the effective charge Q depends on the laser intensity, which provides another coupling mechanism between the atom density n and photon intensity

I . Such coupling, determined by Eqs. (1), (2), (3) and (4), eventually becomes unstable leading to the nucleation of photon bubbles, representing a local increase in the photon number accompanied by a depletion in the atom density [2]. Here we describe the experimental evidence of such an instability. We should note that the photon bubble mechanism differs from the recently observed pattern formation instability in cold atoms [14]. In the former case, optical dipole forces, from far off-resonant light, are coupled to the atomic density distribution, whereas here we rely on quasi-resonant radiation pressure. Moreover, the pattern formation mechanism results from coherent photon transport, whereas in the photon bubble instability light is in the diffusive limit.

Our experiment consists of a magneto-optical trap (MOT) [15], where ^{85}Rb atoms are collected from a dilute vapor at a background pressure of $\sim 10^{-8} \text{ Torr}$. Six independent colling, and trapping, laser beams cross the center of the trap with a beam waist of $w \sim 4 \text{ cm}$, power per beam $P \sim 40 \text{ mW}$ and wavelength $\lambda \sim 780 \text{ nm}$. Since the beams are not retro-reflected we guarantee that the observed instability does not originate from feedback mechanisms [16]. The cooling laser operates on the D2 line of ^{85}Rb ($F = 3 \rightarrow F' = 4$), and is red-detuned by δ , which can be controlled by a double passage through an acousto-optic modulator (AOM), with a frequency tuning precision higher than the transition linewidth, $\Gamma/2\pi \sim 6 \text{ MHz}$. A magnetic field gradient (∇B) with a zero field at the center of the trap generates a spatially dependent Zeeman split of the energy levels, allowing for magneto-optical trapping of the atoms. A finite probability exists

to excite the open transition $F = 3 \rightarrow F' = 3$, which, in turn, is responsible for a ground state change via a spontaneous Raman transition. An additional repump beam, operating on the hyperfine transition $F = 2 \rightarrow F' = 3$ repopulates the $F = 3$ hyperfine ground state, thus allowing the cooling process to continue. The repump detuning is set by searching for the maximum fluorescence signal. We thus obtain a cold cloud with $N \sim 10^{10}$ atoms at $T \sim 100 \mu K$. A CCD camera working at approximately 350 fps collects the fluorescence signal from the cold atoms. In this way we dynamically measure the atomic distribution of the trap, integrated along the line-of-sight of the camera.

The photon bubble instability described here is observed when the cooling beams are tuned very close to the atomic resonance, $\delta = -0.5 \Gamma$, which we keep constant during the entire experiment time. In such conditions, significant photon trapping occurs inside the cold gas and the diffusive approximation in Eq. (1) becomes the appropriate description of the photon density evolution which, in turn, influences the atom dynamics according to Eq. (2), (3) and (4). We have also set the magnetic field gradient to $\nabla B \sim 9 \text{ G/cm}$, although this parameter has no strong influence on the observed atomic dynamics, in contrast with the laser detuning δ , which strongly determines the system behaviour. In Fig. (1) we plot the temporal evolution of a photon bubble instability, where complex atomic motion takes place. Due to density inhomogeneities, localized photon trapping occurs, which grows from the onset of the instability forming bubble-like structures. The growth of these structures is accompanied by a local decrease in the atom density, due to radiation pressure, which eventually leads to the decay of the bubble due to photon losses and the subsequent reestablishment of the local atom density. Such processes occur at a time scale much slower than the typical plasma frequency, as expected from the photon bubble model [2]. To sustain this claim we determined the frequency power spectrum of the atom density fluctuations by averaging the squared amplitude of the Fourier Transforms of the time signals from each pixel of the CCD camera - see Fig. (2). We start by noting that for an high laser detuning, $\delta = -1.5 \Gamma$, we observe isolated frequency peaks. In fact, it has been reported before [12] that for such region of experimental parameters the system undergoes supercritical Hopf bifurcations resulting in self-sustained oscillations in the collective atom dynamics. This scenario is consistent with the red line spectrum in Fig. (2). When tuning the beams closer to the atomic resonance however, the system undergoes a significant transformation and an unforeseen regime of complex atom motion takes place - $\delta = -0.5 \Gamma$, black line in Fig. (2). In this new regime, the frequency power spectrum exhibits broad band components at low frequencies, as expected from dissipative turbulent systems [17]. This indicates a weak turbulent-like evolution of the atom density, char-

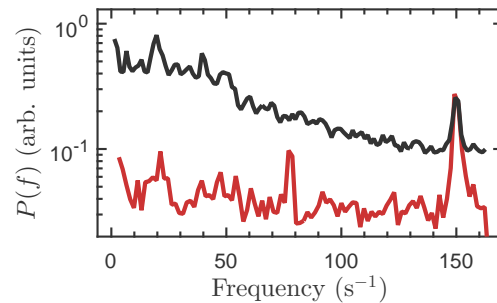


FIG. 2. (color online) The red line represents the power spectrum of the atom dynamics (in the time domain), for a region of parameters ($\delta = -1.5 \Gamma$) where supercritical Hopf bifurcations are observed, resulting in self-sustained oscillations and corresponding to isolated frequency peaks. In the darker line ($\delta = -0.5 \Gamma$) a new dynamical regime is depicted where a characteristic turbulence power spectrum is observed. Broad band components are present at low frequencies, as expected in scenarios of dissipative turbulence - see Discussion.

acterized by fairly well defined dynamical structures, as we are about to demonstrate.

Let us investigate the power spectrum of the density fluctuations, but now in the space domain. We take as many as 500 fluorescence images of the atom cloud, in the experimental conditions described before, yielding the spatial atom distribution integrated along the line-of-sight, which we shall denote by $\bar{n}_i(\rho)$, with $\rho = (x, y)$ and $i = 1, 2, \dots, 500$. From here we compute the mean atom distribution by averaging over the 500 samples, $\bar{n}_0(\rho) = \langle \bar{n}_i(\rho) \rangle$, and subtract to each frame to determine the fluctuating density distributions $\delta \bar{n}_i(\rho) = \bar{n}_i(\rho) - \bar{n}_0(\rho)$. To determine the spectral dependence of the density fluctuations, we Fourier transform each real space distribution $\delta \bar{n}_i(\rho)$ to obtain $\delta \bar{n}_i(\mathbf{k})$. Finally, we can average the squared amplitude of each two-dimensional momentum distribution, $P(\mathbf{k}) = \langle |\delta \bar{n}_i(\mathbf{k})|^2 \rangle$. Note that, assuming isotropic density fluctuations allows us to average the power spectrum in the angular dependence, yielding the desired power spectrum $P(k)$ - see Fig. (3). We shall at this point inquiry about the correctness of taking an integrated distribution and compute the Fourier Transform. The question that naturally arises is if such spectrum does correspond to the real density fluctuations spectrum. The same problem arises, for instance, when investigating turbulence in the inter stellar medium (ISM) [1, 18] from earth-based observations. As it turns out, we can safely take the Fourier Transform of the integrated signal and obtain the correct scaling of the full three dimensional spectral dependence as long as the depth (along the line-of-sight) of the probed medium is at least of the order of the largest transverse scale we are interested in [19, 20].

We shall now discuss the consequences and physical meaning of such a particular k dependence in the density fluctuations spectrum. We start by noting that the

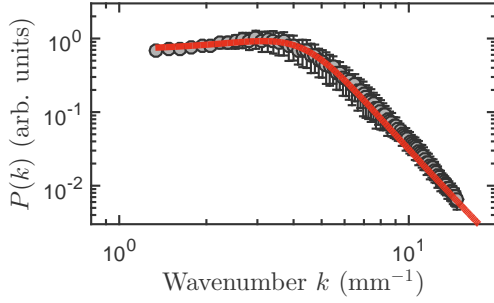


FIG. 3. (color online) Experimental turbulence power spectrum (grey dots). An unusual k^{-4} scaling at high wavenumbers is observed, indicating a fast decay of the density auto-correlation function and revealing the presence of well defined dynamical spatial structures - see Discussion. The error bars correspond to standard deviations when averaging over the angular dependence of the power spectrum. The red line depicts a numerical fit to the theoretical power spectrum derived in Eq. (11).

k^{-4} scaling of the turbulent spectral components corresponds to a much faster decay than the usual Kolmogorov spectrum, $k^{-5/3}$, and other similar turbulence scaling laws. This indicates the existence of structures with well defined scale lengths, and not self-similar or fractal-like structures at different scales. This is easily understood in terms of the auto-correlation function, defined as $C(\delta r) = \langle n(r)n(r + \delta r) \rangle$. Note that, the auto-correlation function $C(\delta r)$ and the power spectrum $P(k)$ are conjugate quantities, forming a Fourier pair. For a scaling of the form $P(k) \sim 1/(a^2 + k^2)^2$, such as we experimentally observe, where a is a regularization at $k \rightarrow 0$ and related with the inverse of a typical scale, the auto-correlation function takes the form $C(\delta r) \sim \exp(-a\delta r)$ with a fast decay at a $1/a$ scale, thus again evidencing the existence of well defined spatial structures with $1/a$ a typical size. This phenomenological analysis will be made more precise in the subsequent discussion.

Let us now investigate to which extent the photon bubble model can account for such particular observations regarding the density fluctuations and the turbulence spectrum. In this sense we must go beyond the linear regime considered in [2]. We begin by assuming slowly growing photon density perturbations described by

$$(\tilde{I}, \tilde{n}) \propto F(\mathbf{r}) e^{-i\Omega t}. \quad (5)$$

Here the mode frequency Ω is much smaller than the effective plasma frequency defined before. Note that non-linear mode saturation can be described by an Helmholtz equation [2] of the form

$$\nabla^2 F(\mathbf{r}) = -q^2 F(\mathbf{r}). \quad (6)$$

The real quantity q determines the scale of the bubble solutions. We should note that Eq. (6) could be derived directly from Eq. (1), (2), (3) and (4), yielding the same

spectral equations. In spherical coordinates $\mathbf{r} = (r, \theta, \phi)$ the solutions are given by

$$F(\mathbf{r}) = j_\ell(qr) Y_{\ell m}(\theta, \phi), \quad (7)$$

where $j_\ell(r)$ are the spherical Bessel functions and $Y_{\ell m}$ the spherical harmonics. We note that such functions may not accurately describe realist photon bubble solutions, as they are perturbed by background fluctuation, such as sound waves, or by photon losses. The erosion associated with lossy processes can be described by a radial absorption length γ , with is related with the damping term γ_a introduced earlier in Eq. (1). More realistic solutions are then given by

$$F(\mathbf{r}) = j_\ell(qr) Y_{\ell m}(\theta, \phi) e^{-\gamma r}. \quad (8)$$

The observed turbulent behavior is described by such solutions, with random angular orientations. The corresponding (radial only) Fourier spectrum, average over randomly oriented spherical harmonics, is given by

$$P_\ell(k) = 4\pi \int_0^\infty j_\ell(qr) e^{-\gamma r} e^{ikr} r^2 dr, \quad (9)$$

where the 4π factor appears from the integration on the angular variables. For the first two modes $\ell = 0$ and $\ell = 1$, we have

$$P_0(k) = \frac{8\pi(\gamma - ik)}{[q^2 + (\gamma - ik)^2]^2}, \quad \text{and} \quad (10)$$

$$P_1(k) = \frac{8\pi q}{[q^2 + (\gamma - ik)^2]^2}, \quad (11)$$

respectively. Notice that, for $k \gg q$, the first mode, corresponding to spherical solutions, decays as k^{-3} while the second mode, corresponding to dipolar-shaped bubbles, decays as k^{-4} . This suggest that we are indeed in the presence of dipolar bubbles. To further clarify the discussion we performed a numerical fit of the absolute value of the expression in Eq. (11) to the experimentally measured power spectrum - see Fig. (3). Here, we can verify the excellent agreement between the theoretical power spectrum and the experiment, over the entire range of accessible wavenumbers. Furthermore, from the numerical fit we can extract the parameters of the model. Particularly, we obtain $q = 3.8 \pm 0.1 \text{ mm}^{-1}$ and $\gamma = 2.2 \pm 0.1 \text{ mm}^{-1}$. Note that the power spectrum attains its maximum for $k \sim q$ and thus $l_0 = 2\pi/q \sim 1.6 \text{ mm}$ corresponds to the typical bubble length scale. As expected $\gamma \lesssim q$, which allows the bubbles to develop and grow.

In conclusion, we demonstrated here that optically thick samples of cold atoms driven close to the atomic resonance can develop photon bubble instabilities due to the strong coupling between the atom density and photon transport, which becomes diffusive due to multiple

scattering inside the medium, under appropriate experimental conditions. Such dynamical structures are at the origin of a distinct low frequency turbulence with a spectrum scaling as k^{-4} , revealing the unsuspected dipolar shape of the bubbles, according to the theory developed here. Photon bubbles have been considered in astrophysical contexts, namely in the atmosphere of neutron stars [21], black hole accretion disks [22, 23] and around young massive stars [24]. Despite previous proposals of laboratory based simulation of such instabilities, namely with high power lasers [25], this is, for the best of our knowledge, the first time photon bubbles resulting from radiation pressure effects are experimentally observed. Radiation pressure is also expected to be at the origin of turbulence in the interstellar medium, with effects in star formation or cosmic-ray propagation [1]. We thus pave the way to investigate complex astrophysical situations with cold atoms experiments.

JR acknowledges the Doctoral Programme in Physics and Mathematics of Information (DP-PMI) and the financial support of FCT - Fundação da Ciência e Tecnologia through the grant number SFRH/BD/52323/2013. HT thanks the support from Fundação para a Ciência e a Tecnologia (Portugal), namely through the programme PTDC/POPH. RK thanks Guillaume Labeyrie for many discussions and experimental insights in large MOTs.

-
- [1] B. G. Elmegreen and J. Scalo, *Annual Review of Astronomy and Astrophysics* **42**, 211 (2004).
 - [2] J. T. Mendonça and R. Kaiser, *Phys. Rev. Lett.* **108**, 033001 (2012).
 - [3] T. Walker, D. Sesko, and C. Wieman, *Phys. Rev. Lett.* **64**, 408 (1990).
 - [4] J. Mendonça, R. Kaiser, H. Terças, and J. Loureiro, *Phys. Rev. A* **78**, 013408 (2008).
 - [5] J. T. Mendonça and H. Terças, *Physics of Ultra-Cold Matter* (Spring Series on Atomic, Optical and Plasma Physics Vol. 70, Berlin, 2012).
 - [6] M. C. W. van Rossum and T. M. Nieuwenhuizen, *Rev. Mod. Phys.* **71**, 313 (1999).
 - [7] A. Ishimaru, *Wave Propagation and Scattering in Random Media* (Academic, New York, 1978).
 - [8] G. Labeyrie, E. Vaujour, C. A. Müller, D. Delande, C. Miniatura, D. Wilkowski, and R. Kaiser, *Phys. Rev. Lett.* **91**, 223904 (2003).
 - [9] L. Pruvost, I. Serre, H. T. Duong, and J. Jortner, *Phys. Rev. A* **61**, 053408 (2000).
 - [10] H. Terças, J. T. Mendonça, and V. Guerra, *Phys. Rev. A* **86**, 053630 (2012).
 - [11] J. D. Rodrigues, H. Terças, and J. T. Mendonça, *EPL (Europhysics Letters)* **113**, 13001 (2016).
 - [12] G. Labeyrie, F. Michaud, and R. Kaiser, *Phys. Rev. Lett.* **96**, 023003 (2006).
 - [13] J. D. Rodrigues, J. A. Rodrigues, O. L. Moreira, H. Terças, and J. T. Mendonça, *Phys. Rev. A* **93**, 023404 (2016).
 - [14] L. G., T. E., G. P. M., O. G.-L., F. W. J., R. G. R. M., A. A. S., K. R., and A. T., *Nat Photon* **8**, 321 (2014).
 - [15] E. L. Raab, M. Prentiss, A. Cable, S. Chu, and D. E. Pritchard, *Phys. Rev. Lett.* **59**, 2631 (1987).
 - [16] D. Wilkowski, J. Ringot, D. Hennequin, and J. C. Garreau, *Phys. Rev. Lett.* **85**, 1839 (2000).
 - [17] J. P. Eckmann, *Rev. Mod. Phys.* **53**, 643 (1981).
 - [18] D. Falceta-Gonçalves, G. Kowal, E. Falgarone, and A. C.-L. Chian, *Nonlinear Processes in Geophysics* **21**, 587 (2014).
 - [19] M.-A. Miville-Deschênes, F. Levrier, and E. Falgarone, *The Astrophysical Journal* **593**, 831 (2003).
 - [20] R. Romain, A. Jallageas, P. Verkerk, and D. Hennequin, *ArXiv e-prints* (2016), [arXiv:1602.06181](https://arxiv.org/abs/1602.06181) [physics.atom-ph].
 - [21] J. Arons, *Astrophys. J.* **388**, 561 (1992).
 - [22] C. F. Gammie, *Monthly Notices of the Royal Astronomical Society* **297** (1998).
 - [23] M. C. Begelman, *The Astrophysical Journal* **643**, 1065 (2006).
 - [24] N. J. Turner, E. Quataert, and H. W. Yorke, *The Astrophysical Journal* **662**, 1052 (2007).
 - [25] S. J. Moon, S. C. Wilks, R. I. Klein, B. A. Remington, D. D. Ryutov, A. J. Mackinnon, P. K. Patel, and A. Spitkovsky, *Astrophysics and Space Science* **298**, 293.